7. M. C. Nuss *et al.*, *IEEE Electron Device Lett.* **11**, 200 (1990).

8. R. N. Simons *et al.*, *IEEE MTT-S International Microwave Symposium Digest*, 915 (1989).

9. R. Majidi-Ahy *et al.*, *IEEE Trans. Microwave Theory Tech.* **38**, 1986 (1990).

10. J. A. Valdmanis, *Electron. Lett.* **23**, 1308 (1987), and references therein.

2.B Angle-Resolved X-Ray Photoemission Study of the Surface Disordering of Pb(100)

A surface atom has a reduced number of nearest neighbors when compared to an atom in the bulk. This enhances the thermal vibrations of the surface atoms, often leading to surface disordering (or surface melting) below the bulk-melting temperature. The temperature-dependent disordering of surfaces can be studied using a variety of surface-sensitive techniques, such as ion shadowing and blocking,[1,2] low-energy electron diffraction (LEED),[3–6] x-ray scattering,[7] and x-ray photoelectron diffraction (XPD).[8] Results have conclusively shown that Pb(110) experiences surface disordering, and the temperatures for the various stages of surface disorder are well established.[1–8] Theoretical analysis has shown that the propensity for surface disorder with temperature depends on packing and is highest for open surfaces.[9] For example, Pb(111) is more densely packed than Pb(110) and is found to resist surface disordering up to the bulk-melting temperature (T_m = 600.7 K). Its temperature dependence has been almost entirely attributed to the Debye-Waller effect, i.e., the intensity attenuation of the diffraction peaks is exponential in temperature.[4] The Pb(100) surface is more closely packed than Pb(110) but less packed than Pb(111). We have found that Pb(100) experiences surface disordering but to a lesser degree than Pb(110).[10] Ion shadowing and blocking has been used to study the temperature-dependent disordering of Pb(100); approximately five disordered layers have been found on Pb(100) at about 600 K.[2] The rate of change of the disordered-layer thickness did not diverge as T_m was approached; thus, it has been suggested that Pb(100) is "on the verge" of surface melting.[2]

In our experiment we used XPD to study the dependence of the forward-scattered intensity of the [001] and [011] azimuths of Pb(100) on temperature. One of the most important characteristics of XPD is its strong forward scattering, i.e., the intensity is enhanced along inter-nuclear axes. The angular-intensity distribution can be used to characterize the degree of surface order.[11,12] For electron energies of several hundred electron volts, multiple scattering defocuses electrons emitted below approximately four atomic layers.[12] Hence, XPD is a highly surface-sensitive probe. We find that Pb(100) experiences an attenuation of the forward-scattered intensity that, above 550±11 K, cannot be explained solely by the Debye-Waller effect. Above 585±5 K, the rate of intensity attenuation increases and we attribute this to the growth of a surface-disordered layer. A slight anisotropy

is seen with the [011] azimuth experiencing a faster decay. By comparing our results along the [001] azimuth with previous experiments on Pb(110),[2,8] we estimate the disordered-layer thickness on Pb(100) to be 4–5 monolayers at 599±0.6 K.

Experiment and Data Analysis

The crystal was oriented within 0.75° of the Pb(100) surface as confirmed by Laue back reflection. The sample was cut with a fine-band saw to twice its final thickness, polished with silicon carbide grit paper, and finally chemically etched in a mixture of 80% glacial acetic acid and 20% hydrogen peroxide (30% in water). Prior to insertion in the ultrahigh vacuum (UHV) chamber, the sample was again chemically etched.

The sample was clipped to a resistively heated molybdenum base mounted on a five-axis manipulator. Two thermocouples monitored the temperature of the front and back surfaces of the sample. Temperature stability was better than ±0.6 K and the maximum temperature difference across the sample was 1 K. Data were taken to within 1.7±0.6 K of T_m. The thermocouples were calibrated to the freezing and boiling temperatures of water, and to the melting temperature of lead by melting the sample *in situ* at the conclusion of the experiment.

Before data acquisition, the sample was cleaned with argon-ion bombardment and annealed to approximately 2 K below T_m until an atomically clean surface was obtained. Oxygen and carbon levels were checked throughout the experiment via x-ray photoelectron spectroscopy (XPS) of the 1s transition for both elements. Auger electron spectroscopy was occasionally used to confirm the XPS results. A Mg Kα x-ray source (E = 1253.6 eV), at 28.8° from the surface normal, provided the incident radiation. The binding energy of the $4f_{7/2}$ core-level photoelectrons is 136.6 eV; therefore, 1117.0-eV electrons were emitted from the lead sample. The scattered electron intensity was detected with a hemispherical energy analyzer mounted on a two-axis goniometer. The resolution of the analyzer as determined by LEED is 1.6° FWHM. The base pressure of the UHV system is $<1 \times 10^{-10}$ Torr. The actual pressure during the experiment was higher because of argon-ion bombardment, the x-ray source, and heating of the sample. Sample orientation was checked with reflection high-energy electron diffraction and LEED. Intensities were recorded at angular steps of 1°.

Electrons with an energy of 1117.0 eV have an estimated inelastic mean-free path λ_{in} of 24 Å in lead.[13–15] This corresponds to a maximum escape depth of 10 monolayers for $\theta = 0°$ and 3 monolayers for $\theta = 72°$, where θ is the angle measured from the surface normal. However, multiple scattering events effectively reduce λ_{in} and must be included to provide accurate predictions.[16] Unfortunately, such calculations are complicated and therefore rarely incorporated in quantitative analysis. Recently, an effective electron mean-free path has been introduced that is affected by both the elastic and inelastic mean-free paths; multiple scattering can be partially accounted for in a single scattering calculation by substituting λ_{eff} for λ_{in},

where $0.5\,\lambda_{in} \leq \lambda_{eff} \leq 0.7\,\lambda_{in}$.[17] The possible dependence of λ_{eff} on crystal direction is still unaccounted for.

Forward-scattered peaks are expected to be visible at 0°, 18.4°, 45°, and 71.6° for the [001] azimuth, and 0°, 19.5°, 35.3°, and 54.7° for the [011] azimuth for a nonrelaxed (100) surface. We analyzed all eight of these peaks. In our polar scans, forward-scattered peaks appear within 1° of these expected values, except for the peak at 71.6° that appears within 2°. Discrepancies may arise from a small error in the spectrometer step size (within ±0.6% of the actual setting), interference effects, multilayer relaxation, and increased refraction for large θ angles.[12] However, multilayer relaxation and refraction effects are ruled out for the peak predicted at 71.6° since both would result in a change opposite to what is observed.[18] In addition, smaller peaks are observed at approximately 32° and 58° for [001] and 68° for [011]. These are due to first-order constructive interference at an off-axis angle, which results when the phase difference between the two paths is 2π.[12]

Our data acquisition was performed in the following manner. Polar scans were taken at 1117.0 eV and at two other energies (1133.6 eV and 1093.6 eV) for which no lead peaks are seen. The latter two polar scans were used to interpolate the background at 1117.0 eV for each value of θ. The background was then subtracted from the raw intensity data. This was completed during data acquisition and we refer to the resulting polar scans as as-acquired data. Further analysis was accomplished as follows. Nonforward-scattered electrons were accounted for by fitting a polynomial to the highest temperature data for each azimuth after the remaining forward scattering was removed. At such high temperatures, the forward-scattered peaks are weak because of surface disordering. The instrumental response was determined from a polar scan at 1133.6 eV that was fit to a polynomial. The data correction was accomplished as follows:

$$I_{corr}(\theta,T) = \frac{I(\theta,T)-I_{bkgd}(\theta,T)}{I_{ir}(\theta,T)}, \qquad (1)$$

where $I(\theta,T)$, $I_{bkgd}(\theta,T)$, and $I_{ir}(\theta,T)$ are the as-acquired data, nonforward-scattered background, and instrumental response given in Fig. 47.26(a), and $I_{corr}(\theta,T)$ is the corrected data shown in Fig. 47.26(b) for the [001] azimuth of Pb(100) at $T = 326\pm0.6$ K. θ is the angle from the surface normal and T is the temperature.

The temperature dependence of the intensity of the forward-scattered peaks $I_{corr}(\theta,T)$ for a given angle can be presented as a plot of $\ln[I_{corr}(\theta,T)]$ versus temperature. Such plots are shown for the [001] azimuth of Pb(100) in Fig. 47.27. The result is a linear dependence up to a particular temperature, which we have found to be 550±11 K for Pb(100), after which $\ln[I_{corr}(\theta,T)]$ diverges from linear behavior at an increasing rate. The line that best fits the data in the linear region is determined using the method of least squares; the number of data points included in the fit is chosen to maximize the statistical correlation coefficient between the line fit and the data. The linear

region, for which the intensity attenuation is exponential in temperature, is attributed to the Debye-Waller effect. At temperatures above 550±11 K, additional phenomena are necessary to describe the observed behavior.

Surface Disordering

The effects of a surface-disordered layer on the forward-scattered intensity are now considered. The intensity is exponentially attenuated with an exponent proportional to $l/\lambda_{eff}\cos\theta$ where l is the thickness of the disordered layer.[8] It has been shown that the disordered layer grows as a function of temperature according to the relation

$$l \sim \ln\left[(T_m - T_o)/(T_m - T)\right], \tag{2}$$

where T_o is the characteristic temperature for the onset of surface disorder.[1,3,8,19] This behavior is expected for a three-dimensional system governed by short-range atomic interactions; such is the case for metals.[2,20] If the disordered-layer thickness exceeds the range of these interactions, long-range forces become important and the disorder grows as a power law.[2] Given the exponential attenuation described above, as well as Eq. (2), the normalized intensity is expected to have the following form:[4,8]

$$I_{corr}(\theta,T)/I_{DW}(\theta,T) = \left[(T_m - T_o)/(T_m - T)\right]^r, \tag{3}$$

where $I_{DW}(\theta,T)$ is the Debye-Waller exponential function obtained from line fits such as in Fig. 47.27 and r is a constant that depends on λ_{eff} and θ.

We account for the Debye-Waller attenuation by dividing $I_{corr}(\theta,T)$ by $I_{DW}(\theta,T)$. In Fig. 47.28, $\ln[I_{corr}(\theta,T)/I_{DW}(\theta,T)]$ is plotted versus $\ln(T_m - T)$. The horizontal region where $\ln[I_{corr}(\theta,T)/I_{DW}(\theta,T)] = 0$ represents Debye-Waller behavior, and the linear region for high temperatures indicates logarithmic growth of the disordered layer. The intermediate temperature region shows a slow intensity attenuation in excess of that predicted by Debye-Waller. We attribute this behavior to partial disordering of the first atomic layer. We interpret the steep linear region at higher temperatures as the spread of disorder to deeper atomic layers. If this line fit is extrapolated to the temperature axis, we find T_o = 585±5 K for the [001] and [011] azimuths. A slight anisotropy is observed; [011] experiences a more rapid decrease in intensity above T_o. Consideration of the solid-liquid interface provides an explanation for the observed anisotropy.[3] The interfacial free energy is lowest in the direction in which the atomic spacing of the solid is closest to the atomic spacing of the liquid. For Pb(100) this occurs along the [011] azimuth. This is consistent with Pb(110) where the $[1\bar{1}0]$ azimuth disorders faster than [100].[3,4,6,8,21]

Using LEED, Prince *et al.*[3] have found T_o = 543±3 K for the [001] and $[1\bar{1}0]$ azimuths of Pb(110). In their experiment, the intensity disappeared into the background above approximately 575 K for $[1\bar{1}0]$ and approached the background for [001]. In an XPD experiment on Pb(110), Breuer and coworkers[8] have observed logarithmic growth of the disordered layer for a

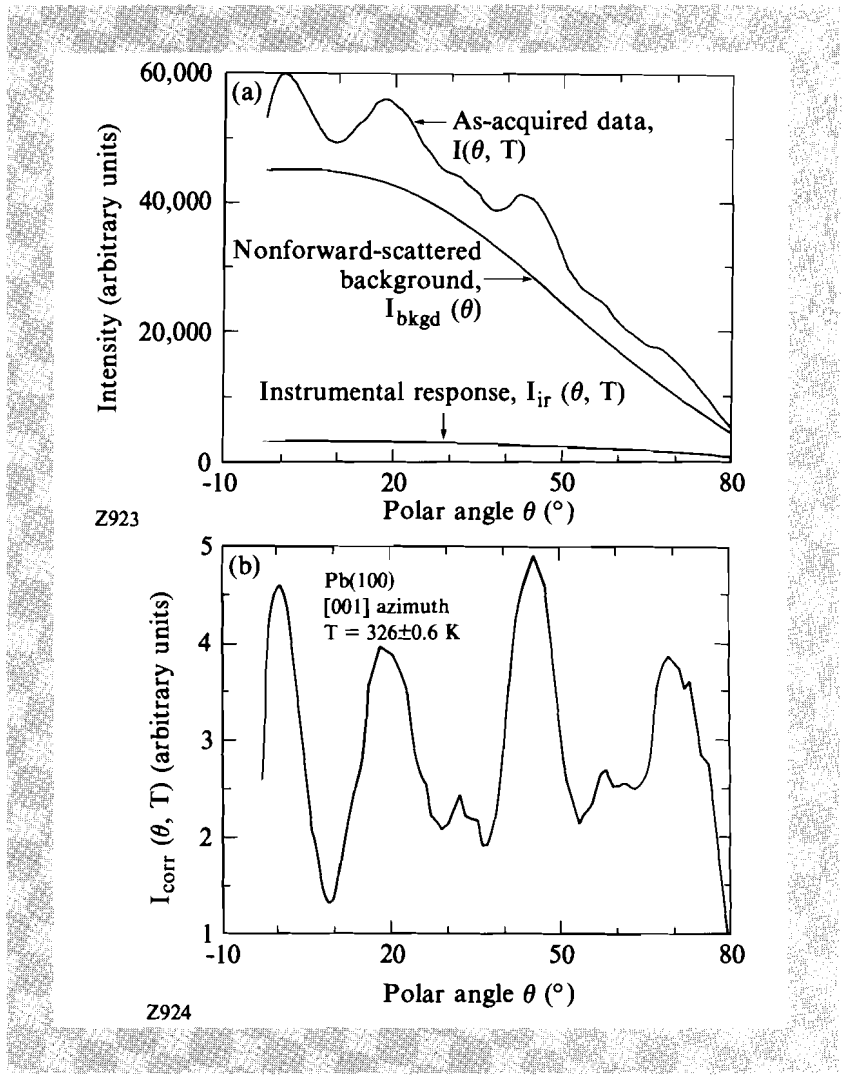

Fig. 47.26
Polar scans are shown for the [001] azimuth of Pb(100) at $T = 326 \pm 0.6$ K: (a) as-acquired data $I(\theta,T)$, nonforward-scattered background $I_{bkgd}(\theta,T)$, and instrumental response $I_{ir}(\theta,T)$. (b) The corrected forward-scattered intensity $I_{corr}(\theta,T)$, obtained using Eq. (1).

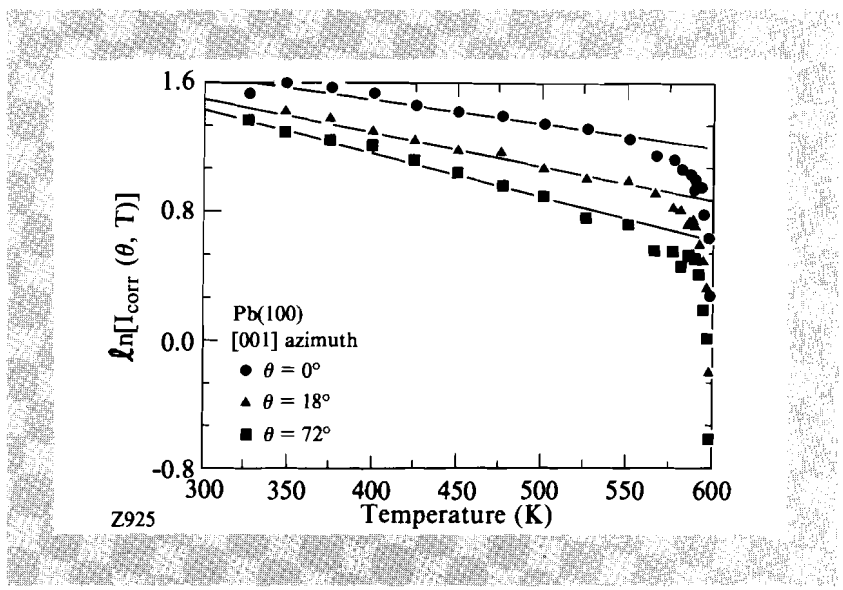

Fig. 47.27
The logarithm of the corrected forward-scattered peak intensity $\ln[I_{corr}(\theta,T)]$ is given as a function of temperature for various angles along the [001] azimuth. The linear region at low temperatures is attributed to the Debye-Waller effect. Deviation from Debye-Waller behavior is seen above 550±11 K.

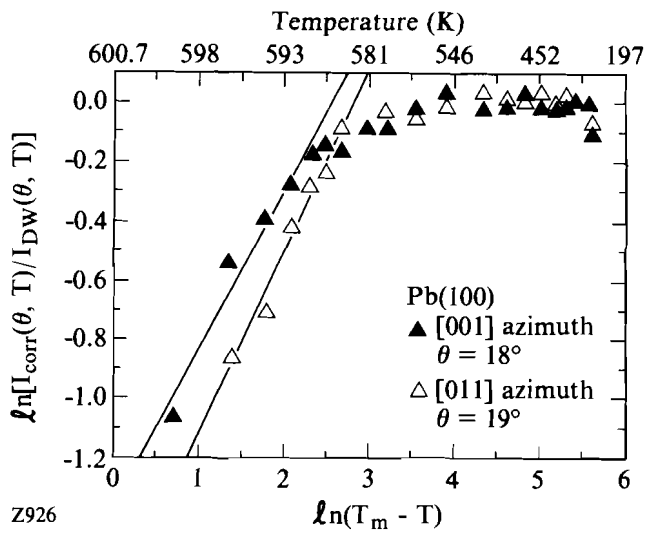

Fig. 47.28
The logarithm of the corrected forward-scattered peak intensity normalized to the Debye-Waller fit $\ln[I_{corr}(\theta,T)/I_{DW}(\theta,T)]$ is plotted versus $\ln(T_m-T)$. The line fit for temperatures above 585±5 K indicates that the disordered layer experiences logarithmic growth. Some anisotropy is seen; the [011] azimuth decays faster with temperature.

temperature region close to T_m. For a lower-temperature region they have reported the existence of another logarithmic growth law. They have concluded that $T_0 = 530 \pm 5$ K, and that the higher-temperature logarithmic-growth law dominated above 575 K. Temperatures for the onset of surface disorder and complete surface melting were found by Frenken *et al.*[1] to be about 545 K and 580 K, respectively, with ion shadowing and blocking.

In contrast to what has been observed on the Pb(110) surface, we find no evidence for a second logarithmic growth law for Pb(100). It is possible that such a growth law does not exist for Pb(100). This would indicate that Pb(100) experiences what is referred to as incomplete surface melting; that is, the rate of change of the thickness of the disordered layer does not diverge as T_m is approached. This is in contrast to complete surface melting where the disordered layer behaves increasingly like the bulk liquid and its thickness diverges as the temperature nears T_m.[21] Another possibility is that a second growth law exists for Pb(100) at temperatures closer to T_m than we have considered in our experiments.

We next consider the temperature dependence of the number of disordered layers for Pb(100). The temperature-dependent attenuation of the forward-scattered intensity peaks for Pb(110) as obtained by XPD[8] is related to the number of disordered layers on the surface as determined by Pluis *et al.*,[2] who used ion shadowing and blocking. Their data are compared to ours in Fig. 47.29. A deviation from Debye-Waller-like behavior is seen for Pb(110) around 500 K, and around 550 K for Pb(100). Two disordered layers have been found through analysis of the $[1\bar{1}0]$ azimuth, on Pb(110) at 550 K, 4 disordered layers at 587 K, and 8 disordered layers at 599.3 K.[2,8] From a comparison of the intensity attenuation of the [001] azimuth of Pb(100) with these results, we estimate the disordered-layer thickness on Pb(100) to be 2 layers at about 590 K, and 4–5 layers at about 599 K. This is in agreement with the previous results where close to 5 disordered layers were visible

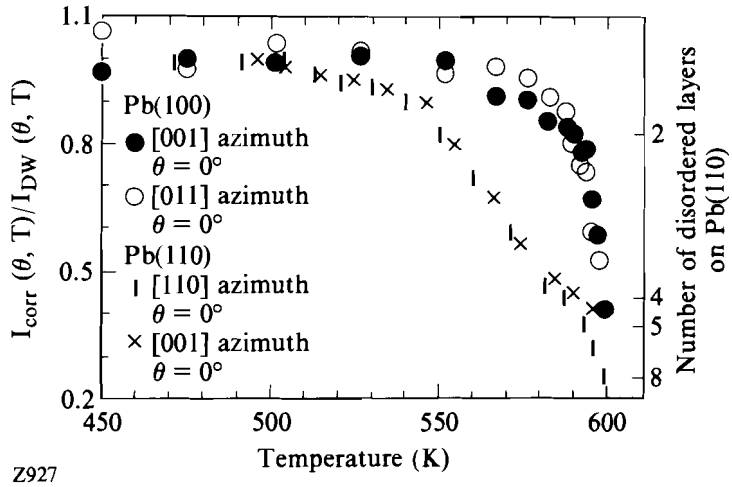

Fig. 47.29
The corrected forward-scattered peak intensities normalized to the Debye-Waller fit $I_{corr}(\theta,T)/I_{DW}(\theta,T)$ is plotted versus temperature for the [001] and [011] azimuths of Pb(100) for $\theta = 0°$. Normalized data for the [001] and [1$\bar{1}$0] azimuths of Pb(110) are from Ref. 8. The number of disordered layers on Pb(110) as a function of temperature from Refs. 2 and 8 are compared to $I_{corr}(\theta,T)/I_{DW}(\theta,T)$ to predict the number of disordered layers on Pb(100).

around 600 K for Pb(100).[2] The forward-scattered peak at 72° for the [001] azimuth of Pb(100) nearly disappears at 599 K, although not completely. Thus, slight order must still exist in the first 3 monolayers at 599 K (3 monolayers is the upper limit of the escape depth at 72°).

The thickness of the disordered layer can also be estimated by considering the attenuation of the forward-scattered peaks by elastic and inelastic scattering. These peaks are assumed to decay exponentially with the disordered-layer thickness:

$$\ln\left[I_{corr}(\theta,T)/I_{DW}(\theta,T)\right] = -l/\lambda_{eff}\cos\theta. \qquad (4)$$

For the [001] azimuth of Pb(100) at 599±0.6 K and $\theta = 0°$, 4.5 to 6.3 disordered layers are predicted for $0.5\,\lambda_{in} \leq \lambda_{eff} \leq 0.7\,\lambda_{in}$.[17]

Conclusion

The [001] and [011] azimuths of Pb(100) exhibit surface disorder below the bulk-melting temperature, although the surface-melting process appears to be incomplete. Intensity attenuation can no longer be attributed to the Debye-Waller effect above 550±11 K. The characteristic temperature for the onset of surface disorder T_o is 585±5 K for both the [001] and [011] azimuths. A slight anisotropy is exhibited; the [011] has a more rapid intensity attenuation for temperatures above T_o. Comparison of our data for the [001] azimuth to previous work suggests that approximately 4–5 disordered atomic layers are present on the Pb(100) surface at 599±0.6 K.

ACKNOWLEDGMENT

This work was supported by the U. S. Department of Energy under contract No. DE-FG02-88ER45376. Additional support was provided by the National Science Foundation under contract No. DMR-8913880 as well as the Laser Fusion Feasibility Project at the Laboratory for Laser Energetics, which is sponsored by the New York State Energy Research and Development Authority and the University of Rochester. We gratefully acknowledge a research fellowship from the Alfred P. Sloan Foundation.

REFERENCES

1. J. W. M. Frenken and J. F. van der Veen, *Phys. Rev. Lett.* **54**, 134 (1985); J. W. M. Frenken, P. M. J. Maree, and J. F. van der Veen, *Phys. Rev. B* **34**, 7506 (1986).
2. B. Pluis *et al.*, *Phys. Rev. Lett.* **59**, 2678 (1987); B. Pluis *et al.*, *Phys. Rev. B* **40**, 1353 (1989); B. Pluis, Ph. D. thesis: *Surface-Induced Melting of Lead*, University of Leiden (1990).
3. K. C. Prince, U. Breuer, and H. P. Bonzel, *Phys. Rev. Lett.* **60**, 1146 (1988).
4. U. Breuer *et al.*, *Surf. Sci.* **223**, 258 (1989).
5. H. N. Yang, T. M. Lu, and G. C. Wang, *Phys. Rev. Lett.* **63**, 1621 (1989).
6. A. Pavlovska, H. Steffen, and E. Bauer, *Surf. Sci.* **234**, 143 (1990).
7. P. H. Fuoss, L. J. Norton, and S. Brennan, *Phys. Rev. Lett.* **60**, 2046 (1988).
8. U. Breuer, O. Knauff, and H. P. Bonzel, *Phys. Rev. B* **41**, 10848 (1990); U. Breuer, O. Knauff, and H. P. Bonzel, *J. Vac. Sci. Technol. A* **8**, 2489 (1990).
9. A. Trayanov and E. Tosatti, *Phys. Rev. B* **38**, 6961 (1988).
10. E. A. Murphy, H. E. Elsayed-Ali, K. T. Park, J. Cao, and Y. Gao, *Phys. Rev. B* **43**, 12615 (1991).
11. W. F. Egelhoff, Jr., *Phys. Rev. Lett.* **59**, 559 (1987).
12. W. F. Egelhoff, Jr., *CRC Crit. Rev. Solid State & Mater. Sci.* **16**, 213 (1990).
13. M. P. Seah and W. A. Dench, *Surf. & Interface Anal.* **1**, 2 (1979).
14. P. Cadman and G. M. Gossedge, *J. Electron Spectrosc. & Relat. Phenom.* **18**, 161 (1980).
15. D. Chadwick, A. B. Christie, and M. A. Karolewski, *Surf. & Interface Anal.* **11**, 144 (1988).
16. S. Y. Tong, H. C. Poon, and D. R. Snider, *Phys. Rev. B* **32**, 2096 (1985).
17. H. P. Bonzel, U. Breuer, and O. Knauff, *Surf. Sci.* **237**, L398 (1990).
18. R. F. Lin, Y. S. Li, F. Jona, and P. M. Marcus, *Phys. Rev. B* **42**, 1150 (1990).
19. R. Lipowsky, *Ferroelectrics* **73**, 69 (1987).
20. J. F. van der Veen, B. Pluis, and A. W. Denier van der Gon, *Chemistry and Physics of Solid Surfaces VII*, edited by R. Vanselow and R. Howe (Springer-Verlag, Berlin 1988), pp. 455–490.
21. R. Lipowsky *et al.*, *Phys. Rev. Lett.* **62**, 913 (1989).